Materials Transactions, Vol. 49, No. 2 (2008) pp. 339 to 344

Novel Bamboo-Like Fibrous, Micro-Channeled and Functional Gradient Microstructure Control of Ceramics

Byong-Taek Lee[1,*], Swapan Kumar Sarkar[1] and Ho-Yeon Song[2,*]

[1]*Department of Biomedical Engineering and Materials, School of Medicine, Soonchunhyang University, 366-1 Sangyoung-dong, Cheonan City, Chungnam 330-090, Korea*
[2]*Department of Microbiology, School of Medicine, Soonchunhyang University, 366-1 Ssangyoung-dong, Cheonan City, Chungnam 330-090, Korea*

In this paper development of novel ceramic microstructures by the fibrous monolithic process were reported. Attempts were made to tailor the microstructures of these advanced ceramics by introducing fibrous or layered morphology to incorporate multi-toughening mechanisms. Fabrication and characterization of four different kinds of microstructure, termed in this manuscript as network type, double network type, functional gradient microchanneled and functional gradient microchanneled double network type microstructure, were reported. In network and double network type microstructure developments the two phase Al_2O_3-(m-ZrO_2) cores were embedded within network-type frames of t-ZrO_2 single phase. In the double network type microstructure, an additional thicker network-type t-ZrO_2 enclosure surrounded a network-type micro-assembly. Unidirectionally aligned continuously porous HAp-Al_2O_3-ZrO_2 tri-phase ceramic composites were fabricated by the same method to incorporated functional gradient for improved functionality and depress processing defects. The microstructure had three layers of HAp/HAp-(Al_2O_3-(m-ZrO_2))/Al_2O_3-(t-ZrO_2) around the continuous pore with compositional gradient. In the functionally gradient micro-channeled HAp/HAp-(Al_2O_3-(m-ZrO_2))/Al_2O_3-(t-ZrO_2) composites, the size and distribution of micro-channels were homogeneously controlled. Detailed morphological analyses of the resulting microstructures were studied. [doi:10.2320/matertrans.MRA2007148]

(Received June 29, 2007; Accepted October 15, 2007; Published January 25, 2008)

Keywords: *ceramics, functionally graded materials, porous material, microstructure*

1. Introduction

During the last two decades, ceramic materials have been used widely in various medical applications such as bone graft substitutes,[1)] hip prostheses[2,3)] and dental materials[4)] as well as in other core industrial applications.[5,6)] When biomaterials are implanted into the human body, they cause some types of reaction with the host tissue. In general, bio-ceramics can be categorized in three possible types depending on the tissue/implant interactions: (1) bio-inert: non toxic to tissue and forms a fibrous capsule around the implant surface,[7)] (2) bioactive: the tissue chemically bonds with the implant surface,[8)] and (3) bio-absorbable: the implant surface dissolves, allowing tissue to refill the space previously occupied by the implant.[9)] Al_2O_3, ZrO_2, and hydroxyapatite (HAp, $Ca_{10}(PO_4)_6(OH)_2$), where the former two are well-known as bio-inert and the later as bioactive ceramics, have been widely used as implant materials. But it has been recognized that their monolithic ceramics exhibit brittleness due to the absence of main fracture toughening mechanisms, which hinders their application in load bearing parts. Therefore, many approaches have been proposed to improve the mechanical properties of monolithic ceramics by using the conventional powder metallurgy process, *i.e.*, the reinforcement is dispersed randomly as a second phase in the matrix.[10–12)] In this case, there were some limitations for homogeneous controlling and tailoring of the microstructure in the common ceramics. In addition, using the common approaches, direct fabrication of fibrous and micro-channeled composites as well as a desirable thin layer coating on the micro-channeled bodies was not possible. Furthermore, ceramic whiskers and fibers pose serious health hazards, were expensive and difficult to achieve homogeneous dispersion in the matrix.[13,14)]

In this work, typical bio-inert ceramics such as Al_2O_3, ZrO_2 and bioactive HAp and their composites were selected based on previous research[6)] for application of bio-ceramics. For application as a bone substitute, porous microstructures are required to give optimal cell-growing conditions. To improve the osteo-conductivity of bio-ceramics, many studies have been reported on the fabrication of porous bio-ceramics as well as a HAp coating on the bio-inert ceramics.[15)] Pore size and porosity were important factors for improving the biocompatibility of bio-ceramics,[16)] as they were closely related to cell attachment, growth behavior and bonding between the bone tissue and the artificial implant in the human body.[17,18)] The suitable pore size for bio-ceramics was reported to be approximately 100–300 μm in diameter.[18,19)]

Recently, an innovative fibrous monolithic process was adapted to impart desirable mechanical properties as well as continuously porous ceramic composites.[20,21)] This newly designed fibrous monolithic process is an effective way to control the bio-mimetic bamboo-like fibrous microstructure.

In the present work, we report on the fabrication of novel microstructures with the aim to improve the material properties and incorporate suitable functionality in the Al_2O_3-ZrO_2 based composites. A range of microstructures with different attributes like fibrous microstructure, microchanneled porosity, *in-situ* coating in the pore with functional gradient etc. was designed and controlled in the aforesaid ceramic material systems. The results can lead to the fabrication of smart materials incorporating unique and desirable features. Using this novel fibrous monolithic process, network-type dense, functional gradient and micro-channeled bodies were fabricated by changing the stacking arrangement of the initial feed roll.

*Corresponding author, E-mail: lbt@sch.ac.kr, songmic@sch.ac.kr

2. Experimental Procedure

2.1 Materials

Alumina (α-Al_2O_3, about 300 nm, AKP-50, Sumitomo, Japan), monoclinic zirconia (m-ZrO_2, about 80 nm, Tosoh Corporation, Nanyo manufacturing complex, Japan), tetragonal zirconia (t-ZrO_2, 3 mol% yttria stabilized zirconia, about 80 nm, Tosoh Corporation, Nanyo manufacturing complex, Japan) Hydroxyapatite (HAp, $Ca_{10}(PO_4)_6(OH)_2$, about 10 μm, Strem Chemicals, Newburyport, MA 01950 USA) and carbon (C, about 20 μm, Aldrich Chemical Company, USA), Ethylene vinyl acetate (EVA) (ELVAX 210 and 250, Dupont, USA) and stearic acid ($CH_3(CH_2)_{16}COOH$, Daejung Chemicals & Metals Co., Korea) were used as starting materials.

2.2 Preparation of extruded and sintered bodies

75 vol% Al_2O_3 and 25 vol% m-ZrO_2 powders were homogeneously mixed in ethanol by ball mill using Al_2O_3 balls as milling media. The mixture was dried on a hotplate while stirring. After that all the materials were separately mixed with polymer binder and stearic acid using a shear mixer (C.W. Brabender Instruments, Shina platech Co., Hwaseong Gyeong-Gi-Do, Korea). The composition of the mixture was controlled in such a way that when extrusion at warm temperature, all the mixtures exhibit almost similar rheological performance. This is vital for the microstructure control of the extruded composites. The particle sizes of the materials were different, so to keep the similar rheological, the mixture composition was finalized as shown in Table 1. In the next step, the t-ZrO_2 and HAp mixtures were used to prepare a tube-like shell by warm press, and the Al_2O_3/m-ZrO_2 and carbon mixtures were used to make a rod-like core. The fabrication method in general is shown in the schematic diagram in Fig. 1(a). In the case of dense network type fibrous Al_2O_3-(m-ZrO_2)/t-ZrO_2 composites, the core of Al_2O_3/m-ZrO_2 mixture and shell of t-ZrO_2 mixture were arranged according to the schematic diagram shown in Fig. 1(b). Extrusion was carried out to get 1st passed filament which was again arranged in the same extrusion die with 61 filaments in the group and extruded to get 2nd passed filament. The 3rd and 4th passed filaments were made with repeating the extrusion in a similar manner. To obtain double network type composites, the core in the initial feed roll was made with a bundle of 1st passed network type Al_2O_3-(m-ZrO_2)/t-ZrO_2 filaments as shown in Fig. 1(c). Extrusion was carried out 4 times to get the final 4th passed filaments.

Table 1 Composition of the shear mixing inputs.

Materials	Solid Vol^m%	Polymer Vol^m%	Stearic acid Vol^m%
t-ZrO_2	47	40	13
Al_2O_3-m-ZrO_2	50	40	10
HAp	50	40	10
Carbon	50	40	10

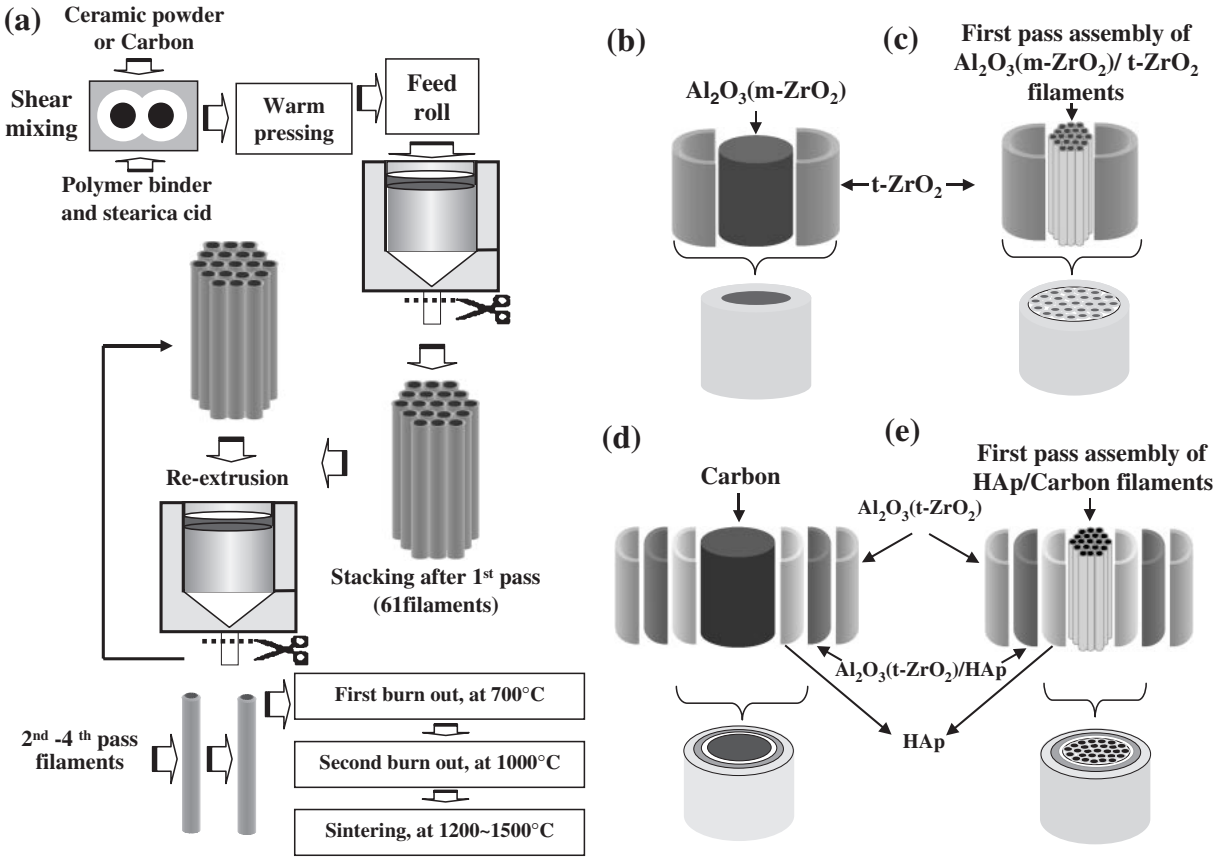

Fig. 1 Schematic diagram of fibrous monolithic process (a); (b) feed roll arrangements for the network type fibrous Al_2O_3-(m-ZrO_2)/t-ZrO_2 composites, (c) double network type fibrous Al_2O_3-(m-ZrO_2)/t-ZrO_2 composites, (d) functional gradient and micro-channeled Al_2O_3-(t-ZrO_2)/HAp composites, (e) double-network type Al_2O_3-(t-ZrO_2)/HAp micro-channeled composites.

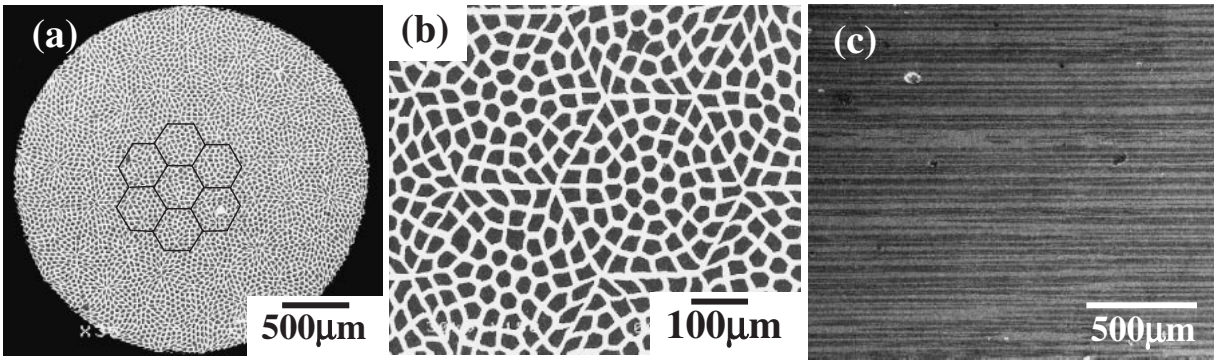

Fig. 2 BSE-SEM images of network type fibrous Al_2O_3-(m-ZrO_2)/t-ZrO_2 composites sintered at 1450°C; (a) cross sectional SEM micrograph, (b) enlarged image of (a), (c) longitudinal SEM micrograph.

However, to make the functional gradient and micro-channeled bodies, the polymer mixed carbon was used as a pore forming agent and two shells (HAp mixtures and Al_2O_3-(t-ZrO_2) mixture) were assembled in the feed roll as shown in Fig. 1(d). In the double network type Al_2O_3-(t-ZrO_2)/HAp micro-channeled composites, the core in the feed roll was assembled with first passed filament of HAp/carbon and the shell was the same as that of functional gradient and micro-channeled bodies. In both of the cases, the extrusion was carried out until 2nd pass.

In the final step, the EVA binder was removed by a burn-out process using a tube furnace in an inert atmosphere up to 700°C. However, for the micro-channeled bodies, as an additional step, the 2nd burn-out process at 1000°C in an air atmosphere was required to remove the pore forming agent (carbon). Finally, samples were sintered in an air atmosphere at different temperature using a pressureless sintering furnace.

2.3 Characterization

The sintered samples were cut and polished using 1 μm of diamond paste. The polished samples were coated with Pt using a vacuum sputter coater. Finally, the detailed micro-structures, phase and crystal structure analysis were observed using a scanning electron microscope (SEM, JSM-635F, Jeol, Japan), EDS (Sirion, FEI, Netherlands) and XRD (XRD, D/MAX-250, Rigaku, Tokyo, Japan), respectively.

3. Results and Discussion

Figure 2 shows the cross sectional and longitudinal sectional SEM micrographs of network-type fibrous Al_2O_3-(m-ZrO_2)/t-ZrO_2 (3 mol% yittria stabilized zirconia) composites sintered at 1450°C. In the low magnification image (a), the Al_2O_3-(m-ZrO_2) cores and t-ZrO_2 network frames were observed with black and white contrasts, respectively. The hexagonal unit indicated by solid lines in Fig. 2(a) was formed during the first extrusion and represents the initial arrangement of filaments. In the enlarged SEM image (b), taken in BSE mode, the hexagonal unit cell and the Al_2O_3-(m-ZrO_2) cores and t-ZrO_2 network frames were clearly observed. In the longitudinal section image (c), the continuously fibrous Al_2O_3-(m-ZrO_2) cores and t-ZrO_2 network frames was seen to be straight, in alternate layers. From this observation, it is confirmed that the novel bamboo-like, fibrous microstructure was well-controlled, using the fibrous monolithic process. This result has remarkably important meaning for the tailoring of the microstructure of advanced materials without dependency on materials (ceramic, metal and polymer systems), chemical composition (oxides and nonoxides) or crystal structure (crystalline and noncrystalline phases), because it is possible to control the desirable microstructures irrespective of the properties of raw powders. The diameter of the Al_2O_3-(m-ZrO_2) cores and the thickness of the t-ZrO_2 network frames were about 30 μm and 10 μm, respectively for the 3rd passed composites. On further increasing of the extrusion pass, the microstructure gets more and more fine and homogenized. After each pass the dimension of the core and shell reduces to about one tenth. However, this also poses a limit for increasing the pass no subsequently because of the particle size of the constituent phases, which must be lower enough compared to the core or shell dimensions. Using ceramic nano powders, this method can fabricate the nanostructured composites with tailored microstructure.

The network type microstructure with finer dimension was shown in Fig. 3. The Al_2O_3-(m-ZrO_2) cores were very fine with less than 4 μm in diameter; whereas the thickness of the continuous t-ZrO_2 network was about 1 μm. Figure 3(b) shows the enlarged SEM image of the interface region between the Al_2O_3-(m-ZrO_2) core and t-ZrO_2 network. In the core region, Al_2O_3 and m-ZrO_2 grains were clearly observed with dark and bright contrasts, respectively. The Al_2O_3 grains could not undergo significant grain growth due to the presence of the m-ZrO_2. It was reported in our previous work[10] that the presence of m-ZrO_2 in the Al_2O_3 matrix imparted microcracks in the grain boundary due to the difference of the thermal expansion coefficients. These microcracks can act as energy dissipator during the crack propagation and improve the fracture toughness. Moreover, observation of superplasticity was reported in alumina doped with zirconia.[22] So, the inclusion of m-ZrO_2 phase in the alumina core can attribute these desirable features. The EDS profiles 'c', 'd' and 'f' were taken from the marked 'c', 'd' and 'f' in Fig. 3(b) which correspond to Al_2O_3, m-ZrO_2 and t-ZrO_2 phases, respectively.

In our second approach, we modified the microstructure of the ceramic systems with micro group of network type

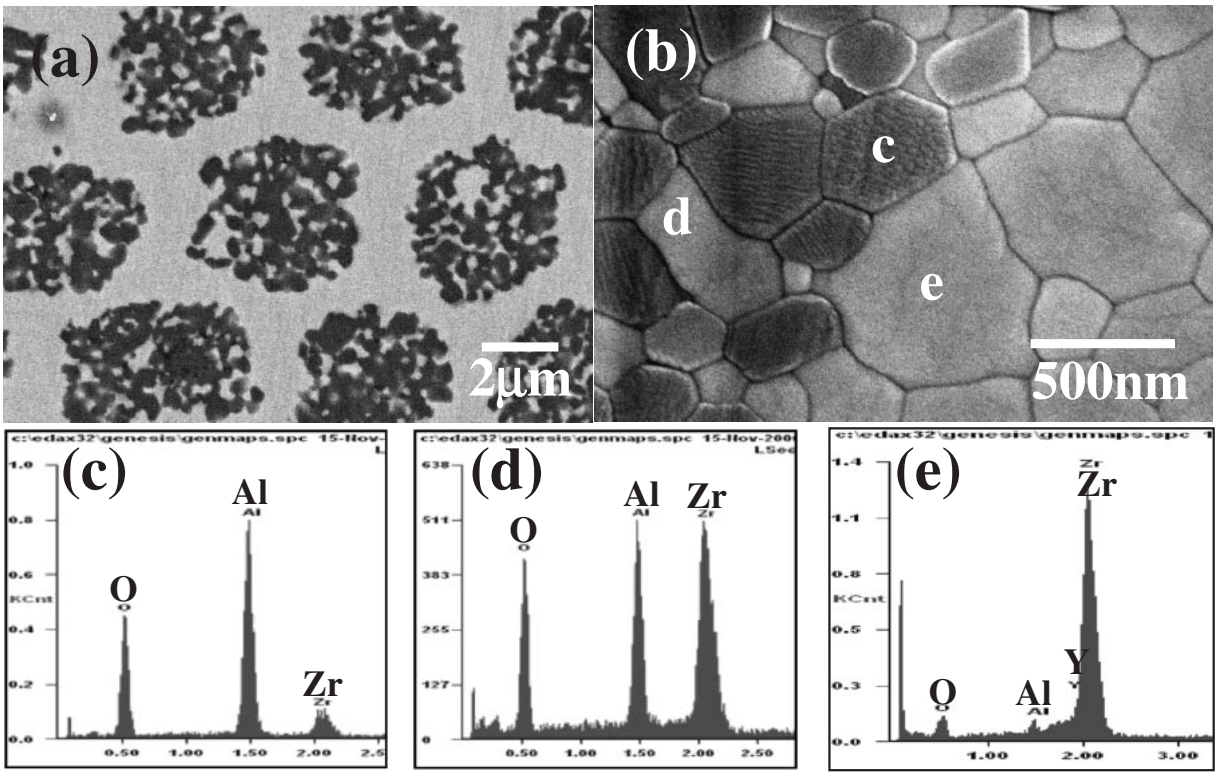

Fig. 3 SEM images of network type fibrous Al_2O_3-(m-ZrO_2)/t-ZrO_2 composites sintered at 1450°C; (a) cross sectional SEM micrograph, (b) enlarged image of the interface and (c–e) EDS profiles taken from c, d and e regions as marked in Fig. (b).

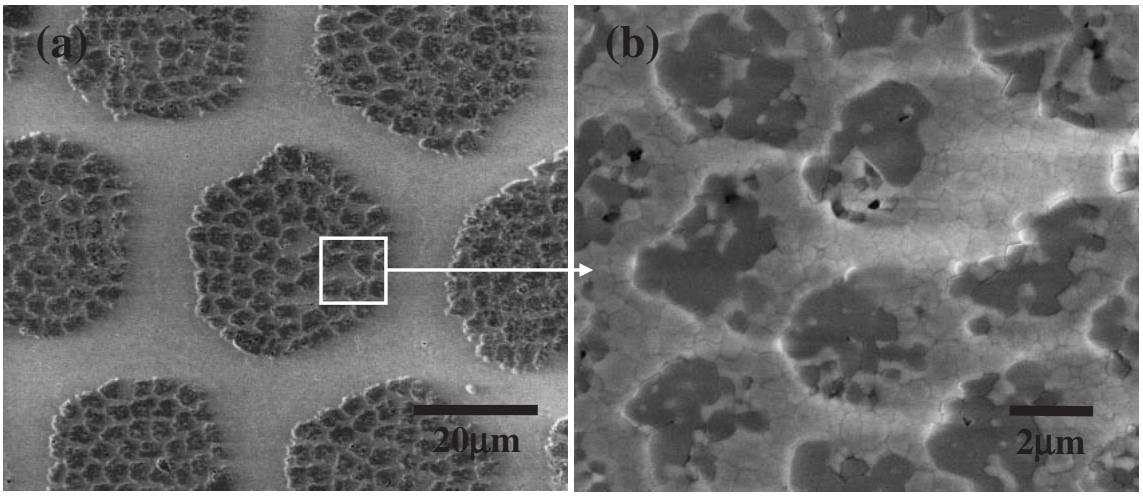

Fig. 4 SEM images of double-network type fibrous Al_2O_3-(m-ZrO_2)/t-ZrO_2 composites sintered at 1500°C; (a) SEM image of 4th passed composites and (b) Enlarged SEM image of passed cross sectional SEM micrographs.

formation encapsulated in another larger dimension network type assembly. Thus a novel double-network type microstructure was fabricated. Figure 4 shows the cross sectional SEM micrographs of the double-network type fibrous (Al_2O_3-m-ZrO_2)/t-ZrO_2 composites sintered at 1500°C. In the low magnification image 4 (a), double-network type fibrous (Al_2O_3-m-ZrO_2)/t-ZrO_2 composites were clearly observed with a fine control of microstructure. The network type microstructure was perfectly controlled with thick outer (10 μm) and thin inner (0.7 μm) t-ZrO_2 network type frames and Al_2O_3-(m-ZrO_2) cores encapsulated in the inner network of t-ZrO_2. In Fig. 4(b) the enlarged image shows this more clearly. The outer network maintained a hexagonal shape while the inner network was somewhat irregular. It is to be noted that the inner network received 5 times of extrusion where the outer network received 4 times extrusion as can be understood from Fig. 1(c). These hexagonal unit cells were formed during the second extrusion to obtain the 2nd passed filaments from the assembly of the 1st passed filaments. The hexagonal geometry of the unit cell depends primarily on the arrangement of the green filament in the extrusion die and as well as on the die geometry.

In Fig. 5 the longitudinal images of the double network type composites are shown. In Fig. 5(a) we can see the

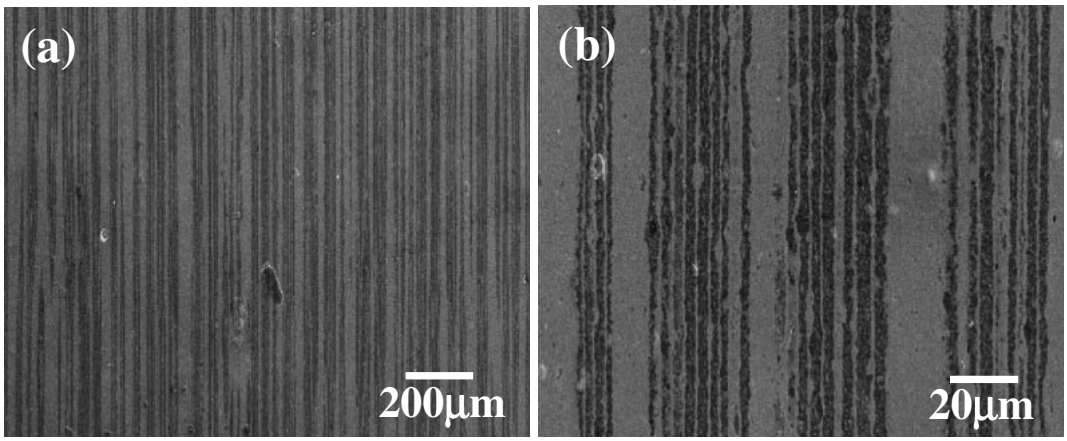

Fig. 5 SEM images of (a) longitudinal section of double-network type fibrous Al_2O_3-(m-ZrO_2)/t-ZrO_2 composites sintered at 1500°C and (b) is the enlarged image taken from (a).

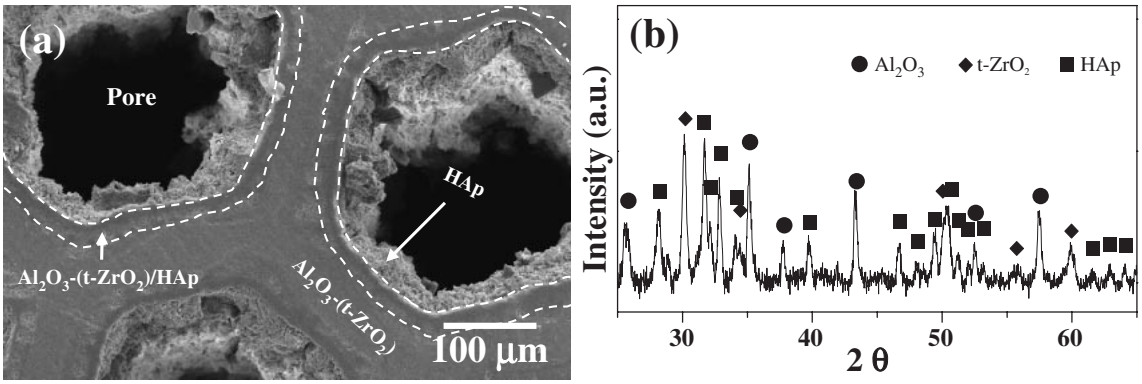

Fig. 6 SEM images of functional gradient and micro-channeled composites sintered at 1200°C (a). (b) XRD profile of the system.

microstructure is unidirectionally aligned. The outer t-ZrO_2 network is seen as the white contrast. However, to see the network type micro groups, the enlarged image Fig. 5(b) was taken. In the figure we can see the inner micro groups with very fine unidirectional alignment.

The coefficient of thermal expansion (CTE) of HAp and Al_2O_3-25% ZrO_2 composite are $13 \times 10^{-6\circ}C^{-1}$ and $6.88 \times 10^{-6\circ}C^{-1}$, respectively. Thus, during the sintering process of Al_2O_3-(t-ZrO_2)/HAp composites, bulk defects such as microcracks and delamination could be formed due to the mismatch of their CTE values which can lead to the formation of cracks and flaws near the interface. In the fabrication of porous composites this can be much more prolific. In our approach to fabricate the microchanneled composites of Al_2O_3-(t-ZrO_2)/HAp by the fibrous monolithic process, we overcome these restraining possibilities by incorporating functionally gradient layer of ceramics. To avoid the bulk defects at the interfaces between HAp and Al_2O_3-(t-ZrO_2) phases, the composites were designed with functional gradient 3 layers, *i.e.*, HAp, HAp/Al_2O_3-(t-ZrO_2) and Al_2O_3-(t-ZrO_2). Figure 6(a) shows the SEM micrographs of micro-channeled Al_2O_3-(t-ZrO_2)/HAp sintered bodies in which micro-channeled frames consist of 3 functional gradient layers and with average pore size of 180 μm in diameter. The functional gradient 3 layers (HAp, HAp/Al_2O_3-(t-ZrO_2) and Al_2O_3-(t-ZrO_2) were clearly observed as indicated by dotted lines. No bulk defects such as cracks or delamination were found. From the XRD profile Fig. (b), it was confirmed that HAp phase still existed without phase transformation of β-TCP because of the comparatively low temperature sintering at 1200°C. On the other hand, Figure 7(a) shows the double-network type and micro-channeled Al_2O_3-(t-ZrO_2)/HAp composites. In Fig. 7(b) the magnified image showed different layers in the microstructures in which the outer network frames had a functional gradient composition (HAp, HAp/Al_2O_3-(t-ZrO_2), Al_2O_3-(t-ZrO_2)) marked by 'P', 'Q' and 'R', respectively and the inner frame was monolithic HAp marked by 'S'. The pore size was about 100 μm in diameter.

As mentioned above, the novel fibrous monolithic process has a remarkable potential for controlling the microstructure of advanced materials. To realize the huge potential functions of advanced materials, the processing factors should be optimized and carefully controlled. The fibrous monolithic processing conditions such as ram speed, loads, temperature of dies and die design, are understood as key factors to develop sound microstructures. Furthermore, the burn-out conditions (duration, heating rate, temperature level and atmosphere) also can be critical factors to perfectly remove the polymer binders as well as to eliminate the bulk defects such as swelling and cracking. In this paper, we reported how novel bamboo-like fibrous, micro-channeled and functionally gradient advanced materials can be fabricated. Because pore control technology has been recognized as a key-issue in

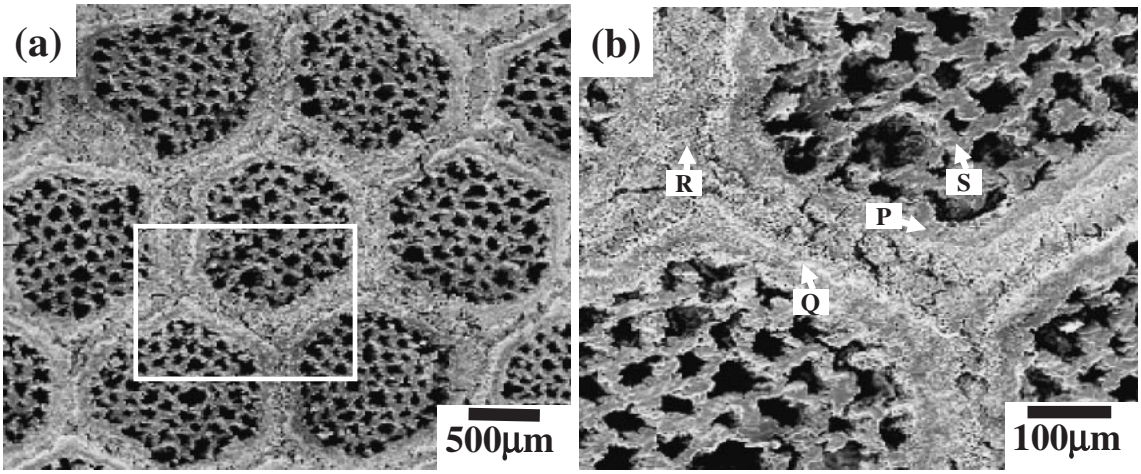

Fig. 7 SEM images of functional gradient and micro-channeled double-network type Al_2O_3-(t-ZrO_2)/HAp composites.

overcoming common limitations of some material properties,[23] the novel fibrous monolithic process can be widely used in the development of advanced materials.

4. Conclusions

Novel microstructures in both dense and porous composites with unidirectional fibrous and functional gradient types were fabricated by the fibrous monolithic process. The versatility of fabrication of various microstructures along with the flexible control on the dimensions and shapes of the microstructure was demonstrated with four types of Al_2O_3-ZrO_2 based composites. In the dense composites, network type and double network type microstructures were fabricated without large size bulk defects. On the other hand in the porous composites, the functionally gradient composites were fabricated with network type and double network type microstructures. The micro-channels in the composites were designed in such a way that they pose the ability to be used as advanced materials.

Acknowledgement

This work was supported by the Regional Innovation Center (RIC) of Sooncunhyang University under the support Korea Foundation Grant funded by Government of Korea (Regional Inovation Center Promotion Fund, MOCIE-RIC060605).

REFERENCES

1) D. Stubbs, M. Deakin, P. Chapman-Sheath, W. Bruce, J. Debes, R. M. Gillies and W. R. Walsh: Biomater. **25** (2004) 5037–5044.
2) N. J. Hallab, C. Messina, A. Skipor and J. J. Jacobs: J. Orthop. Res. **22** (2004) 250–259.
3) S. A. Maher and P. J. Prendergast: J. Biomechanics **35** (2002) 257–265.
4) D. E. Ruddell, J. Y. Thompson and B. R. Stoner: J. Biomed. Mater. Res. **51** (2000) 316–320.
5) G. D. Zhan, J. D. Kuntz, J. Wan and A. K. Mukherjee: Nature Mater. **2** (2003) 38–42.
6) B. T. Lee, K. H. Kim and J. K. Han: J. Mater. Res. **19** (2004) 3234–3241.
7) C. R. Rambo and H. Seiber: Adv. Mater. **17** (2005) 1088–1091.
8) J. M. Comez-Vega, E. Saiz, A. P. Tomsia, T. Oku, K. Suganuma, G. W. Marshall and S. J. Marshall: Adv. Mater. **12** (2000) 894–898.
9) W. Suchanek, M. Yashima, M. Kakihana and M. Yashima: Biomater. **18** (1997) 923–933.
10) B. T. Lee and K. Hiraga: J. Mater. Res. **9** (1994) 1199–1207.
11) Y. Jia, Y. Hotta, K. Sato and K. Watan: J. Am. Ceram. Soc. **89** (2006) 1103–1106.
12) B. N. Kim, K. Hiraga, K. Morita and Y. Sakka: Acta Mater. **49** (2001) 887–895.
13) G. L. Vaughan, J. Jordan and S. Karr: Environmental Res. **56** (1991) 57–67.
14) W. L. Suchanek and M. Yoshimura: J. Am. Ceram. Soc. **81** (1998) 765–767.
15) A. K. Gain and B. T. Lee: J. Am. Ceram. Soc. **89** (2006) 2051–2056.
16) S. H. Kwon, Y. K. Jun, S. H. Hong, I. S. Lee and H. E. Kim: J. Am. Ceram. Soc. **85** (2002) 3129–3131.
17) B. T. Lee, I. C. Kang, S. H. Cho and H. Y. Song: J. Am. Ceram. Soc. **88** (2005) 2262–2266.
18) L. L. Hench: J. Am. Ceram. Soc. **81** (1998) 1705–1728.
19) K. A. Hing, S. M. Best and W. Bonfield: J. Mater. Sci. Mater. Med. **10** (1999) 135–145.
20) R. K. Paul, A. K. Gain, H. D. Jang and B. T. Lee: J. Am. Ceram. Soc. **89** (2006) 2057–2062.
21) A. K. Gain, H. Y. Song and B. T. Lee: Scrip. Mater. **54** (2006) 2081–2085.
22) Z. C. Wang, T. J. Davies, N. Ridley and A. A. Ogwu: Acta Mater. **44** (1996) 4301–4309.
23) A. Zimmermann, M. Hoffman, B. D. Flinn, R. K. Bordia, T. J. Chuang, E. R. Fuller Jr. and J. Rodel: J. Am. Ceram. Soc. **81** (1998) 2449–2457.